Chapter 2:

A Distinct Mechanism to Achieve Efficient SRP–SRP Receptor Interaction by the Chloroplast SRP Pathway

A version of this chapter has been published as:

Jaru-Ampornpan, P., Nguyen, T. X., and Shan, S. (2009) *Mol. Biol. Cell*, **20** (7), 3965–3973.

Abstract

Co-translational protein targeting by the signal recognition particle (SRP) requires the SRP RNA, which accelerates the interaction between the SRP and SRP receptor 200-fold. This otherwise universally conserved SRP RNA is missing in the chloroplast SRP (cpSRP) pathway. Instead, the cpSRP and cpSRP receptor (cpFtsY) by themselves can interact 200-fold faster than their bacterial homologues. Here, cross-complementation analyses revealed the molecular origin underlying their efficient interaction. We found that cpFtsY is five–tenfold more efficient than *E. coli* FtsY at interacting with the GTPase domain of SRP from both chloroplast and bacteria, suggesting that cpFtsY is pre-organized into a conformation more conducive to complex formation. Further, the cargo-binding M-domain of cpSRP provides an additional 100-fold acceleration for the interaction between the chloroplast GTPases, functionally mimicking the effect of the SRP RNA in the co-translational targeting pathway. The stimulatory effect of the SRP RNA or the M-domain of cpSRP is unique to each pathway. These results strongly suggest that the M-domain of SRP actively communicates with the SRP and SR GTPases, and that the cytosolic and chloroplast SRP pathways have evolved distinct molecular mechanisms (RNA vs. protein) to mediate this communication.

Introduction

The signal recognition particle (SRP) and the SRP receptor (SR) comprise the major cellular machineries that co-translationally deliver newly synthesized proteins from the cytosol to target membranes (*1*, *2*). Co-translational protein targeting begins with recognition of the cargo—ribosomes translating nascent polypeptides containing signal sequences—by the SRP (*3*). The cargo is brought to the vicinity of the target membrane via the interaction between the SRP and SRP receptor (FtsY in bacteria) (*4*). Upon arrival at the membrane, SRP unloads its cargo to the protein-conducting channel, composed of the sec61p complex (or secYEG complex in bacteria) (*5*–*7*). The SRP and SRP receptor also reciprocally stimulate each other's GTPase activity (*8*). Thus after cargo unloading, GTP hydrolysis drives disassembly of the SRP•SR complex, returning the components into the cytosol for the next round of protein targeting (*9*).

The SRP pathway is conserved throughout all three kingdoms of life. Although the protein components of SRP and SR vary across species, the functional core of SRP is a highly conserved ribonucleoprotein complex, conprised of a 54-kD SRP GTPase (SRP54 in eukaryotes or Ffh in bacteria) and an SRP RNA (*2*). The SRP receptor also contains a conserved GTPase domain that is highly homologous to the GTPase domain in SRP54, and together the GTPase domains of SRP and SR form a unique subgroup in the GTPase superfamily (*2*). Both proteins contain a central GTPase "G" domain that adopts the classical *Ras*-type GTPase fold (*10*, *11*). Unique to the SRP family of GTPases is an N-terminal extension, termed the "N" domain, that forms a four-helix bundle (*10*, *11*). The N- and G-domains form a structural and functional unit called the NG-domain. In addition to the GTPase domains, the SRP and SR proteins contain unique effector

domains that allow them to carry out their biological functions. SRP has a C-terminal extension, a methionine-rich "M" domain, which interacts with the SRP RNA (*12*) and with the signal sequence of the cargo (*13*) SR has an N-terminal extension, an acidic "A" domain, which interacts with the target membrane (*14*) and potentially with the sec translocon (*15*).

SRP and SR form a complex with one another directly through their GTPase domains, and reciprocally activate each other's GTPase activity within the complex (*8*). Both structural and biochemical analyses suggested that these GTPases undergo major structural rearrangements during complex formation (*16, 17*). One of the important conformational changes involves the intra-molecular rearrangement at the interface between the N- and the G-domains (*16–18*). Two conserved motifs at the N–G domain interface, "ALLEADV" on the N-domain and "DARGG" on the G-domain, act as a fulcrum that mediates the re-positioning of the N-domain relative to the G-domain in both SRP and SR (*17*). In addition, an inhibitory element from the first helix of the N-domain is removed (*19*). These structural rearrangements bring the two N-domains into close proximity with one another, allowing them to make additional interface contacts that stabilize the complex (*18*) (*17*). After a stable SRP•SR complex is formed, additional conformational rearrangements occur in both GTPase active sites to activate GTP hydrolysis within the complex (*20*).

A novel SRP-dependent protein targeting pathway has been found in chloroplast (*21*). A unique feature of the cpSRP pathway is that it utilizes a post-translational mode of targeting. Instead of recognizing ribosome•nascent chain complexes as cargo, the cpSRP recognizes light-harvesting chlorophyll-binding proteins (LHCPs) that are

imported into the chloroplast as fully synthesized proteins, and delivers LHCPs from the chloroplast stroma to the thylakoid membrane (*22*, *23*). Analogous to the cytosolic SRP pathways, the cpSRP pathway is mediated by two GTPases, cpSRP54 and cpFtsY, that are close homologues of the cytosolic SRP54 and SR GTPases, respectively. Intriguingly, the other strictly conserved component of the cytosolic SRP pathway, the SRP RNA, has not been found in the cpSRP pathway. Instead, a novel 43-kD protein, cpSRP43, binds to a unique C-terminal extension in cpSRP54, and together the cpSRP43•cpSRP54 complex constitute the chloroplast SRP (*24*). Although early models suggested that cpSRP43 might act as a functional homologue of the SRP RNA to regulate the GTPase activity of the chloroplast SRP and SRP receptor (see below; (*25*)), kinetic analyses showed that cpSRP43 does not considerably affect either the complex formation or GTP hydrolysis rates of cpSRP54 and cpFtsY (*26*). Instead, cpSRP43 interacts specifically with the cargo, the LHCPs, to facilitate substrate recognition (*23*).

In cytosolic SRP pathways, complex formation between the SRP and SR GTPases is extremely slow, presumably because it is limited by the extensive conformational changes required to form a stable complex (*27*, *28*). The SRP RNA overcomes this problem by enhancing the association rate between the two GTPases 200-fold, bringing the SRP–SR interaction rate to a range appropriate for their biological function (*29*). Moreover, the SRP RNA accelerates the rate at which the SRP•SR complex hydrolyzes GTP five–tenfold (*27*, *30*). Many reports have suggested that the SRP RNA may play a regulatory role by bridging the communication between cargo binding and the GTPase cycle (*12*, *31*, *32*). The SRP RNA therefore plays a crucial role

in the SRP pathway, explaining why it is highly conserved from bacteria, archaea, to eukaryotes.

How does the chloroplast SRP bypass such a key component? Previous kinetic analyses revealed that in the absence of the SRP RNA, the association kinetics between cpSRP54 and cpFtsY is 200-fold faster than that of their *E. coli* homologues, and matches the rate of the RNA-stimulated interaction between bacterial SRP and SR (*26*). This provides a simple explanation for the absence of the SRP RNA in the cpSRP pathway, but also raises additional questions. What governs the kinetics of interaction between the SRP and SR GTPases? How can the chloroplast GTPases interact much more efficiently than their bacterial homologues despite their high sequence homology? The crystal structure of apo-cpFtsY shows that, compared to free bacterial FtsY, the conformation of apo-cpFtsY is closer to that observed in the Ffh•FtsY complex, suggesting that some of the N–G rearrangement is already in place in cpFtsY prior to complex formation (*33*). This and additional biochemical results led to a model in which cpFtsY is pre-organized in a conformation that is more conducive to interaction with its binding partner, and thus bypasses some of the conformational changes that limit the rate of association between the bacterial SRP and SR GTPases.

In this work, we present additional evidence for this model by showing that cpFtsY is intrinsically five–tenfold more efficient at interacting with the SRP GTPase. More importantly, we found that the cargo-binding M-domain of cpSRP54, without the help from the SRP RNA, provides an additional ~ 100-fold stimulation in complex formation between the cpSRP and cpFtsY GTPases. Both of these factors allow the chloroplast SRP and SR GTPases to achieve the same efficiency of interaction as the

RNA-catalyzed interaction between their bacterial homologues. The stimulatory effects of the SRP RNA and the M-domain of cpSRP54 are specific to their homologous binding partners and not interchangeable across species, suggesting that the classical and the cpSRP pathways have diverged to use different molecular mechanisms to mediate the communication between the M-domains and the GTPase modules.

Materials and Methods

Protein expression and purification. *E. coli* Ffh and FtsY (47-497) were expressed and purified as described (*27*). The coding sequence of *E. coli* Ffh NG (1-295) was cloned into pET 28b (Novagen) between NcoI and XhoI restriction sites. The recombinant protein, with a His_6 tag at the C-terminus, was expressed in BL21 DE3* (Invitrogen) and purified using Ni-NTA affinity column (Qiagen). *E. coli* Ffh NG (1-295) was further purified by cation exchange over a MonoS column (GE Healthcare) using a linear gradient of 150–600 mM NaCl. FtsY (47-497) interacts with Ffh with the same kinetics as either full-length FtsY or FtsY-NG (Supplementary Figure 2.S1), thus the large A-domain in *E. coli* FtsY does not affect the interaction between the SRP and SR GTPases.

cpSRP54 and cpFtsY were expressed and purified as described (*26*). Mutations of cpFtsY were introduced using the QuikChange Mutagenesis protocol (Stratagene). cpFtsY G288W was purified using the same procedure as that for the wild-type protein. cpFtsY F71V and F71A were purified from inclusion bodies as described (*33*). The coding sequence of cpSRP54 NG (1-294 of the mature protein) and a His_6 tag at the C-terminus was cloned into pAcUW51 (BD Biosciences) between BamHI and HindIII restriction sites. The resulting plasmid was then used for protein expression from baculovirus at the Protein Expression Center of Caltech. The recombinant cpSRP54 NG-His_6 was purified by affinity chromatography using Ni-NTA twice.

To construct the domain swap mutant proteins, pDMF6 encoding *E. coli* Ffh (*10*) was modified to contain an EcoRI site before the start of the Ffh M domain. The plasmid encoding FfhNG-cpSRP54M was constructed by replacing the sequence of FfhM (residues 296-453) with a PCR fragment encoding the cpSRP54M (residues 296-488)

using the EcoRI and BamHI restriction sites. The chimeric protein was expressed in Rosetta competent cells (Novagen) and purified using the same procedure as that for the wild-type Ffh protein (*27*).

Kinetics. All GTPase assays were performed at 25 °C in assay buffer [50 mM KHEPES (pH 7.5), 150 mM KOAc, 2mM $Mg(OAc)_2$, 2mM DTT, 0.01% Nikkol, 10% glycerol]. GTP hydrolysis reactions were followed and analyzed as described (*27*). The reciprocally stimulated GTPase reaction between SRP and SR was determined in multiple turnover reactions ([GTP] >> [E]). The concentration dependence of the observed rate constant (k_{obsd}) is fit to eq 1, in which k_{cat} is the rate constant at saturating SR concentrations, and K_m is the concentration of SR that gives half the maximal rate.

$$k_{obsd} = k_{cat} \times \frac{[SR]}{K_m + [SR]} \qquad \textbf{(1)}$$

In these measurements, the basal GTPase rates from FtsY or cpFtsY were determined in side-by-side experiments (Supplementary Table 2.S1) and subtracted from the rates of the stimulated GTPase reactions prior to data analysis. The rate constants k_{cat}/K_m are listed in Table 2.1. The measurements that are directly compared were performed in side-by-side experiments. The figures show representative data, and Table 2.1 shows the average values from three or more measurements.

Gel filtration chromatography. Complex formation was carried out in column buffer [50 mM KHEPES (pH 7.5), 200 mM NaCl, 2 mM $Mg(OAc)_2$, 2 mM DTT]. For cpFtsY mutants (Figure 2.2C and 2.2D), 2 nmols of cpSRP54 and cpFtsY variants were mixed in

the presence of 450 μM GppNHp and the mixture was incubated on ice for 5 minutes before being loaded onto Superdex 200 (GE Healthcare). For experiments in Figure 2.4 and 2.5 nmols of either cpSRP54 or cpSRP54 NG was mixed with equimolar cpFtsY in the presence of 450 μM GppNHp. The mixture was incubated on ice for specified periods of time before being loaded onto Superdex 200. The identities of the peaks were confirmed by reference runs of the individual proteins.

Results

To better understand the molecular mechanism by which the chloroplast SRP and SR GTPases achieve the same association kinetics as their bacterial homologues without the help from the SRP RNA, a series of cross-complementation experiments were carried out in which we tested the ability of the bacterial SRP receptor to interact with the cpSRP GTPase, and vice versa. The first goal of these experiments is to determine whether the core GTPase modules of SRP and SR, which comprise the heterodimer interface, are conserved across different species. The second goal is to identify unique molecular determinants in each pathway that allow the two different pairs of SRP and SR to efficiently interact with one another.

cpFtsY is intrinsically faster than* E. coli *FtsY at interacting with the SRP GTPase.

We first asked how well the core GTPase domains from the *E. coli* and chloroplast pathways are conserved. To this end, we tested whether the SRP and SRP receptor GTPases can interact with one another across different species. The SRP and SRP receptor reciprocally stimulate the GTPase activity of each other, providing a convenient assay to monitor complex formation between the two GTPases (*27*). In this assay, the observed rate constant of GTP hydrolysis is monitored as a function of SR concentration. The slope of the initial linear portion of the concentration dependence represents the rate constant of the reaction: ^{GTP}•SRP + SR•^{GTP} → products (k_{cat}/K_m), and the rate at saturating SR concentrations (k_{cat}) represents the GTP hydrolysis rate once the complex is formed. For the *E. coli* GTPases, k_{cat}/K_m is equal to the association rate constant between SRP and SR during complex formation (*27*). For the chloroplast

GTPases, this rate constant provides a lower limit for the association rate constant between cpSRP54 and cpFtsY to form an active complex (*26*). In situations where the value of k_{cat} is comparable, the differences in k_{cat}/K_m reflect differences in either the rate or stability of complex formation. Therefore for the analyses below, we used the k_{cat}/K_m values as indices to compare the relative ability of the SRP and SR GTPases to form a complex with their binding partners.

The SRP and SRP receptors from both systems can cross-react with their heterologous binding partners. The chloroplast SRP receptor cpFtsY can interact with the *E. coli* SRP GTPase Ffh (Figure 2.1A, closed circles) and with the isolated NG-domain of Ffh (Ffh NG; Figure 2.1B, closed circles), with rate constants similar to those with its homologous partner, the NG-domain of cpSRP54 (cpSRP54 NG; Figure 2.1C, closed circles and Table 2.1). Analogously, in the absence of the SRP RNA, the *E. coli* SRP receptor FtsY can interact with its heterologous partner cpSRP54 NG (Figure 2.1C, open circles) with rates similar to those with its homologous partners, Ffh and Ffh NG (Figure 2.1 A and B, open circles). Therefore, the core GTPase modules of SRP and SRP receptor from the two pathways are largely conserved and interchangeable.

An interesting observation from the results in Figure 2.1 is that, in all three cases, cpFtsY is more efficient at interacting with the SRP GTPases than *E. coli* FtsY. When the binding partner is cpSRP54 NG, the k_{cat}/K_m value for cpFtsY is fivefold above that for *E. coli* FtsY (Figure 2.1C and Table 2.1). Even with the heterologous partners, *E. coli* Ffh and Ffh NG, cpFtsY exhibits about tenfold faster k_{cat}/K_m over that of *E. coli* FtsY (Figure 2.1 A and B, and Table 2.1). As the GTPase rates at saturating FtsY concentrations (i.e., k_{cat}) are within twofold of each other for FtsY compared to cpFtsY,

these differences in k_{cat}/K_m values stem primarily from differences in complex formation. Further, the basal GTPase rates of cpFtsY and FtsY are similar to one another and are at least 200-fold slower than the stimulated reaction rates (Supplementary Table 2.S1), indicating that the higher reactivity of cpFtsY over FtsY observed in Figure 2.1 reflects a higher efficiency of complex assembly with cpFtsY. These results provide independent evidence for the previously proposed model that cpFtsY is pre-organized in a conformation that is more conducive to interaction with the SRP GTPases than bacterial FtsY. This effect partly explains why cpSRP54 and cpFtsY can efficiently interact with one another in the absence of the SRP RNA (*26*, *33*).

What are the molecular features in cpFtsY that allow it to interact more efficiently with the SRP GTPases? Complex formation requires the rearrangement of the N-domain relative to the G-domain. Previous crystallographic analyses suggest that, compared to bacterial FtsY, the relative position of the G- and N-domains in cpFtsY is more similar to that in the structure of the Ffh•FtsY complex (*33*). This may arise, in part, from the tighter packing interactions at the N–G domain interface, especially between the conserved ALLVSDF and SARGG motifs (highlighted in green and blue, respectively, in Figure 2.2A). In cpFtsY, the aromatic ring of Phe71 from the ALLVSDF motif inserts into the core of the N-domain and packs against the SARGG motif (Figure 2.2A). Phe71 is uniquely conserved among chloroplast FtsYs and is replaced by smaller residues in other species. We probed the importance of this packing by mutagenesis. Mutation of cpFtsY Phe71 to valine, its corresponding residue in *E. coli* FtsY, reduces the interaction rate of cpFtsY with cpSRP54 sixfold (Figure 2.2B, green circles). Mutating this residue to Ala reduces the rate even further (~ eightfold; Figure 2.2B, green squares). The

conserved SARGG motif also contributes significantly in the domain–domain packing interaction, as mutation of the universally conserved Gly288 to a bulky tryptophan is detrimental, reducing the value of k_{cat}/K_m 76-fold (Figure 2.2B, blue). None of these mutations significantly reduce the basal GTPase activity of cpFtsY (Supplementary Table 2.S1), indicating that the observed defects are specific to the interaction of cpSRP54 with cpFtsY.

To provide additional evidence that these mutations impair complex formation between cpSRP54 and cpFtsY, we directly measured complex formation using gel filtration chromatography. SRP and SR GTPases form a stable complex in the presence of GppNHp, and the complex can be separated from the monomers by Superdex 200 (Figure 2.2C; (*34*)). With wild-type cpFtsY efficient complex formation with cpSRP54 was observed, whereas with mutant cpFtsY G288W no detectable complex formation could be found during gel filtration chromatography analysis (Figure 2.2C). Mutant cpFtsY F71V also exhibits a defect in complex formation (Figure 2.2D); the smaller defect of cpFtsY F71V than cpFtsY G288W in the gel filtration analysis is consistent with the less severe reduction of this mutant in k_{cat}/K_m in the GTPase assay. Together, these results demonstrate that the packing interaction at the N–G domain interface is important for the formation of the SRP•SR complex and possibly gives rise to the advantage of cpFtsY in interacting with the SRP GTPases.

The M-domain of cpSRP54 accelerates cpSRP54–cpFtsY association.

The results above demonstrate that the higher reactivity of cpFtsY over *E. coli FtsY* contributes five–tenfold to the 200-fold more efficient association between cpSRP

and cpFtsY in the absence of the SRP RNA (Figure 2.1). We hypothesized that the remaining 50–100-fold effect could arise from cpSPR54, in particular its unique M-domain that interacts with cpSRP43 instead of the SRP RNA.

To test this hypothesis, we compared the interaction rate of cpSRP54 with that of cpSRP54 NG. Remarkably, full-length cpSRP54 exhibits ~ 100-fold faster association kinetics (k_{cat}/K_m) compared to the isolated NG-domain of cpSRP54 (Figure 2.3A, open squares vs. circles). Thus, the M-domain of cpSRP54 can act as a functional mimic of the SRP RNA and accelerates the interaction between the cpSRP54 and cpFtsY GTPase domains. The effect of the M-domain is specific to the interaction between the two chloroplast GTPases, as the basal GTP binding and hydrolysis activity of cpSRP54 NG is indistinguishable, within experimental errors, from that of full-length cpSRP54 (Supplementary Table 2.S1).

The faster k_{cat}/K_m value in the presence of cpSRP54 M-domain implies that the M-domain accelerates the kinetics of protein association between cpSRP54 and cpFtsY. This conclusion is confirmed independently by gel filtration chromatography. With full-length cpSRP54, complex formation is very fast, as the peak representing the cpSRP54•cpFtsY complex is clearly visible as soon as the two proteins are mixed together (Figure 2.4A, black). Complex formation is close to completion within 5 minutes, with less than 40% of cpFtsY remaining in the monomer form (Figure 2.4A, red). In contrast, complex formation is much slower in the case of cpSRP54 NG (Figure 2.4B). Only about 5% of cpFtsY went into the complex after an hour of incubation (Figure 2.4B, red). Qualitatively, these results provide additional evidence that the M-domain of cpSRP54 stimulates complex formation between cpSRP54 and cpFtsY.

The stimulatory effect of the cpSRP54 M-domain is most intriguing in light of the fact that *E. coli* Ffh exhibits similar interaction kinetics with FtsY regardless of whether its M-domain is present **(**Figure 2.3B; (*31*, *33*)). The interaction between the *E. coli* GTPases is only stimulated when the M-domain binds the SRP RNA (Figure 2.3B, (*27*)). The SRP RNA, however, does not affect the kinetics of cpSRP54–cpFtsY association (Figure 2.3B). In summary, the results in this section demonstrate that in both the bacterial and chloroplast SRP pathways, the cargo-binding M-domain of SRP communicates with the GTPase domains and stimulates the interaction between the SRP and SR GTPases. These results also suggest that each pathway has evolved unique molecular mechanisms (RNA vs protein) to achieve this communication (see more below).

The M-domains of SRP specifically communicate with their homologous receptors in each pathway.

The SRP RNA stimulates the association kinetics between bacterial Ffh and FtsY ~ 200-fold. The results above showed that the M-domain of cpSRP54 stimulates complex formation between the cpSRP and cpFtsY GTPases. We next asked whether the effects of the SRP RNA and the M-domain of cpSRP54 are interchangeable between the two pathways, as the core NG-domains of these proteins can interact with the heterologous partners (Figure 2.1). We therefore tested whether the SRP RNA can exert its stimulatory effect in reactions containing cpFtsY, and analogously, whether the M-domain of cpSRP54 can exert its stimulatory effect in reactions containing *E. coli* FtsY.

Using the GTPase assay in this mix-and-match experiment, we systematically analyzed the effect of the SRP RNA and the M-domain of cpSRP54 on the two different SRP receptors. With *E. coli* Ffh, the association rate between Ffh and FtsY is stimulated 376-fold by the SRP RNA (Figure 2.5A, open vs. closed circles; (*27*)). In contrast, there is less than twofold difference when the binding partner is cpFtsY instead of *E. coli* FtsY (Figure 2.5A inset, open vs. closed squares and Table 2.1). These results suggest that cpFtsY, unlike *E. coli* FtsY, lacks the ability to respond to the SRP RNA bound to Ffh. Similarly, when cpFtsY interacts with its homologous partner cpSRP54, the SRP RNA does not provide any rate acceleration (Figure 2.5B, open vs. closed squares, and Figure 2.3B). The SRP RNA has no effect on the interaction of *E. coli* FtsY either when paired with cpSRP54 (Figure 2.5B). These results are expected in light of recent work that demonstrates that cpSRP54 does not bind the bacterial SRP RNA ((*35*); P. J.-A. and S.S., data not shown).

On the other hand, the cpSRP54 M-domain only exerts a stimulatory effect on reactions containing its homologous binding partner cpFtsY (Figure 2.3A). With *E. coli* FtsY as the binding partner, no difference in the association rate is observed for cpSRP54 compared to cpSRP54 NG (Figure 2.5C and Table 2.1). Thus, *E. coli* FtsY lacks the ability to communicate with and respond to the M-domain of cpSRP54.

If the M-domain of cpSRP54 can act as an independent structural unit to stimulate complex formation with cpFtsY, then fusion of the cpSRP54 M-domain to the NG domain of Ffh should stimulate the interaction of Ffh-NG with cpFtsY. To test this possibility, we constructed a chimeric protein, FfhNG-cpSRP54M, by replacing the M-domain of Ffh (including the linker between the G- and M-domains) with that of

cpSRP54. As predicted, the chimeric protein containing the M-domain from cpSRP54 forms an active complex with cpFtsY with a rate constant (k_{cat}/K_m) that is ~ 15-fold faster than Ffh NG (Figure 2.6A, circles vs. squares). This stimulation is specific to the interaction between the two GTPases, as the basal GTPase activity of the fusion protein is similar to those of Ffh NG or Ffh (Supplementary Table 2.S1). This is in contrast to *E. coli* Ffh in which the Ffh M-domain does not appreciably affect the interaction of its NG-domain with cpFtsY (Table 2.1). Unfortunately, the effect of the SRP RNA could not be tested in the reciprocal fusion protein, cpSRP54 NG-Ffh M, as the RNA binding motif in the Ffh M-domain of this chimeric protein does not appear to be well formed and has lost the ability to bind the SRP RNA ($K_d \geq 10$ μM; P. J.-A. and S.S., data not shown).

The stimulation induced by the cpSRP54 M-domain in the chimeric protein is specific to cpFtsY, as the fusion protein interacts with *E. coli* FtsY at the same rate as Ffh NG does (Figure 2.6B, circles vs. dashed line; Table 2.1). Further, the interaction of the chimeric protein with *E. coli* FtsY is 100-fold slower than its interaction with cpFtsY (Figure 2.6B, circles vs. dotted line). If no stimulation arises from the M-domain of cpSRP54, only a five–tenfold rate difference between the reactions of cpFtsY and *E. coli* FtsY would be expected (see Figure 2.1). Thus the M-domain of cpSRP54, even when fused to the GTPase domain from a cytosolic SRP, can provide a 10–20-fold stimulation of interactions with cpFtsY. The extent of stimulation by the cpSRP54 M-domain is ~ fivefold smaller in the fusion protein than in native cpSRP54, suggesting that there are additional inter-domain communications between the M- and NG-domains of cpSRP54 that helps position the M-domain for interacting with cpFtsY that cannot be perfectly captured in the fusion protein. Nevertheless, the results with the fusion protein provide

additional support for the model that the M-domain of cpSRP54 acts as a functional mimic of the SRP RNA and kinetically regulates the interaction between the cpSRP54 and cpFtsY GTPases.

Discussion

Two major differences exist between the cytosolic and chloroplast SRP pathways. First, the cytosolic and chloroplast SRPs recognize significantly different forms of "cargo". The cytosolic SRP interacts with ribosomes•nascent chain complexes bearing SRP signal sequences (*3*, *36*), whereas the cpSRP binds to its substrates, LHCPs, as fully translated proteins (*22*, *23*). Second, the cpSRP lacks the SRP RNA which is otherwise universally conserved in all the other SRP pathways. Instead, the cpSRP consists of the cpSRP54 GTPase and a novel protein only found in chloroplast, cpSRP43 (*21*). Previously, we showed that cpSRP54 and cpFtsY can form a complex with one another at rates 200-fold faster than that of their bacterial homologues, therefore bypassing the requirement for the SRP RNA (*26*). Here, we underscored the molecular mechanisms underlying the large difference in interaction rates between the bacterial and chloroplast SRP and SR GTPases.

Previous biochemical and structural works have suggested a model in which the conformational rearrangement at the N–G domain interface required for SRP–SR complex formation is partly achieved in free cpFtsY, thus allowing it to interact more efficiently with its binding partner cpSRP54 (*26, 33*). In this work, we provide independent biochemical support for this model by showing that cpFtsY is five–tenfold more efficient at interacting with the GTPase domain of SRP, even when the binding partner is the heterologous *E. coli* Ffh (Figure 2.1). Mutational analyses further supported the importance of the domain arrangement in cpFtsY, especially at the N–G domain interface, to the formation of the cpSRP54•cpFtsY complex ((*33*) and this work). These results, along with the previous work, support the model that cpFtsY is pre-

organized in a conformation that allows it to better interact with the GTPase domain of SRP.

Even with the higher reactivity of cpFtsY, the isolated GTPase domains of SRP and SR interact very slowly. For the *E. coli* SRP and SR GTPases, their interaction rate is accelerated 200-fold by the SRP RNA. Intriguingly, we found here that the M-domain of cpSRP54 acts as a functional mimic of the SRP RNA, stimulating the interaction between cpSRP54 and cpFtsY ~ 100-fold. This, together with the higher reactivity of cpFtsY, allows cpSRP54 and cpFtsY to achieve the same interaction rate as the RNA-catalyzed interaction between the bacterial SRP and FtsY, and alleviates the otherwise strict requirement for the SRP RNA in cytosolic SRP pathways. These results, together with previous work, provide strong evidence that the cargo-responding domains of the SRPs from both bacterial and chloroplast systems communicate with the GTPase domains and kinetically regulate complex formation between the SRP and SR GTPases (*37*).

It is interesting to note that, while the GTPase modules (the NG-domains) of SRP and SR can interact with their heterologous binding partners across species, the effects exerted by the M-domains or the SRP RNA are not interchangeable. The stimulatory effect of the SRP RNA or the M-domain of cpSRP54 during complex formation can only be attained when the homologous binding partners are paired together. The SRP RNA can only exert its stimulatory effect during the interaction of *E. coli* Ffh with *E. coli* FtsY. Analogously, the M-domain of cpSRP54 can only exert its stimulatory effect during the interaction of cpSRP54 or the chimeric protein (Ffh NG-cpSRP54 M) with cpFtsY. This specificity implies that the two pathways have evolved distinct mechanisms to mediate

communication between the M- and the GTPase domains. In cytosolic SRP pathways, the SRP receptor has evolved to establish a specific communication with the SRP RNA. Conversely, in the cpSRP pathway, the cpFtsY has evolved to establish a specific communication with the M-domain of cpSRP54.

How does the SRP RNA or the cpSRP54 M-domain stimulate complex formation between the SRP and SR GTPases? Although the detailed molecular mechanism remains unclear, three possible models can be envisioned based on previous and this work. First, the SRP RNA helps to pre-position the Ffh NG-domain such that it is more active at interacting with FtsY (*37*). By analogy, the M-domain of cpSRP54 might pre-position the NG-domain of cpSRP54. Second, the SRP RNA positions the M-domain of Ffh and allows it to transiently interact with the SRP or SR GTPase during complex formation (*38*), whereas in cpSRP54 the M-domain itself is properly positioned to establish these interactions. Third, the two pathways use distinct mechanisms to stimulate complex formation. The SRP RNA may provide a direct tether that holds the cytosolic SRP and SR GTPases together during complex formation (*29*), whereas cpSRP54 could use its M-domain to provide this tether. Our data appear to favor the third possibility. This is because the *E. coli* SRP, even though its M- and NG-domains would be pre-positioned by the SRP RNA, cannot efficiently interact with the chloroplast SRP receptor. Analogously cpSRP54, even though its M- and NG-domains would be pre-positioned, cannot efficiently interact with the *E. coli* FtsY. The stimulatory effect of the SRP RNA and the M-domain of cpSRP54 are highly specific to their homologous receptors, arguing against the first two models, in which the origin of the stimulatory effect would be more generic. These data also suggest that response elements must exist in the GTPases that specifically

interact with the SRP RNA in the case of cytosolic SRP or with the cpSRP54 M-domain in the case of the chloroplast SRP.

It was recently shown that in cytosolic SRP pathways, the SRP RNA exerts its stimulatory effect on SRP-SR complex assembly only in the presence of cargo or stimulatory detergents such as Nikkol that partially mimic the effect of the cargo (*32*, *39*). This led to the proposal that the SRP RNA acts as a molecular linker that turns on the GTPase cycles of SRP and SR in response to signal sequence binding in the M-domain. Similarly, we found that the stimulatory effect of the cpSRP54 M-domain on the cpSRP54-cpFtsY interaction is also dependent on the presence of the stimulatory detergent Nikkol (Supplementary Figure 2.S2). This suggests that, analogous to the cytosolic SRP, the stimulatory effect of the cpSRP54 M-domain on complex formation between the chloroplast SRP and SR GTPases might occur only in response to binding of its cargo LHCP. Thus the M-domain of cpSRP54 might have also subsumed the function of the SRP RNA as a molecular linker that bridges the communication between cargo binding and SRP–SR complex formation.

Acknowledgements

We thank the members of the Shan laboratory for helpful comments on the manuscript. This work was supported by NIH grant GM078024 to S.S. S.S. was supported by the Burroughs Wellcome Fund career award, the Beckman Young Investigator award, and the Packard and Lucile award in science and engineering. P.J.-A. was supported by a fellowship from the Brey Endowment foundation.

Table 2.1 Summary of the k_{cat}/K_m, k_{cat}, and K_m values

SRP GTPase construct	SRP receptor	SRP RNA	k_{cat}/K_m (10^6 M^{-1} min^{-1})	$(k_{cat}/K_m)^{rel}$	k_{cat} (min^{-1})	K_m (μM)
Ffh NG	FtsY	–	0.06 ± 0.01	0.4	4.2±1.3	68±11
	cpFtsY	–	0.74 ± 0.18	5	3.6±1.5	5.8±3.9
Ffh	FtsY	–	0.16 ± 0.01	(1)	5.1±1.3	32±10
	FtsY	+	60.1 ± 11.7	376	57.3±7.5	1.0±0.3
	cpFtsY	–	1.77 ± 0.18	11	5.1±1.4	3.0±0.7
	cpFtsY	+	2.70 ± 0.56	17	9.0±2.4	3.9±1.3
cpSRP54 NG	FtsY	–	0.06 ± 0.01	0.2	29.5±0.7	494±62
	cpFtsY	–	0.31 ± 0.09	(1)	25.1±6.4	85±28
cpSRP54	FtsY	–	0.06 ± 0.01	0.2	17.6±0.6	256±0.7
	FtsY	+	0.06 ± 0.01	0.2	19.7±0.5	260±14
	cpFtsY	–	35.2 ± 9.60	114	55.5±16	1.9±0.5
	cpFtsY	+	23.5 ± 7.78	76	31.7±2.9	1.4±0.3

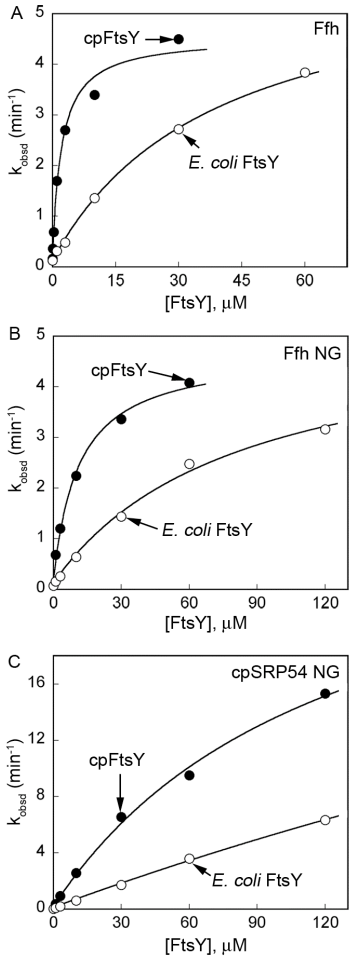

Figure 2.1 cpFtsY is intrinsically faster than *E. coli* FtsY at interacting with the SRP GTPases. Rate constants for the stimulated GTPase reactions were determined with 500 nM Ffh, Ffh NG, or cpSRP54 NG, and with varying concentrations of cpFtsY or *E. coli* FtsY in the presence of 200 μM GTP. (A) Reactions of *E. coli* Ffh with cpFtsY (●) or with *E. coli* FtsY (○). The data were fit to eq 1 and gave a k_{cat} value of 4.4 min^{-1} and a K_m value of 2.2 μM for cpFtsY, and a k_{cat} value of 6.0 min^{-1} and a K_m value of 39 μM for *E. coli* FtsY. (B) Reactions of *E. coli* Ffh NG with cpFtsY (●) or with *E. coli* FtsY (○). The data were fit to eq 1 and gave a k_{cat} value of 4.6 min^{-1} and a K_m value of 10 μM for cpFtsY, and a k_{cat} value of 5.1 min^{-1} and a K_m value of 75 μM for *E. coli* FtsY. (C) Reactions of cpSRP54 NG with cpFtsY (●) or with *E. coli* FtsY (○). The data were fit to eq 1 and gave a k_{cat} value of 30 min^{-1} and a K_m value of 120 μM for cpFtsY, and a k_{cat} value ≥ 16 min^{-1} and a K_m value of 200 μM for *E. coli* FtsY. The values of k_{cat}/K_m are listed for comparison in Table 2.1.

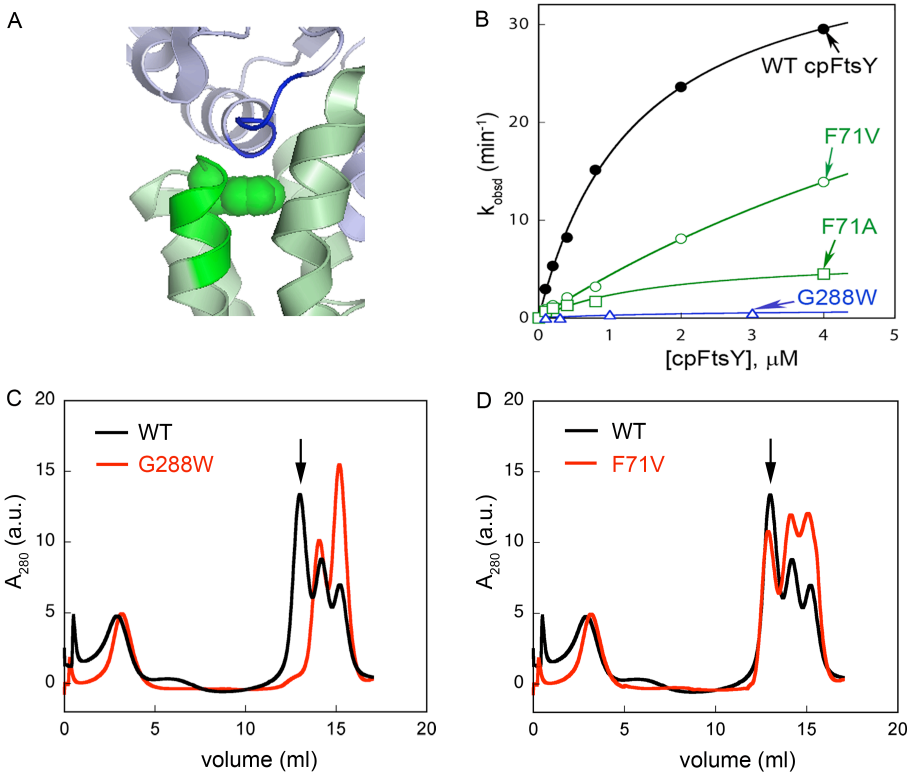

Figure 2.2 Mutations at the N–G domain interface disrupt formation of the cpSRP54•cpFtsY complex. (A) The N–G domain interface of cpFtsY (PDB 2OG2). The G-domain is shown in pale blue, and the N-domain is shown in pale green. The conserved ALLVSDF and SARGG motifs are highlighted in darker shades of green and blue, respectively. F71 (green) is highlighted in space-filled representation. (B) Rate constants for the stimulated GTPase reactions of cpSRP54 with wild type cpFtsY (●), cpFtsY F71V (green circles), cpFtsY F71A (green squares), or cpFtsY G288W (blue triangles). The data were fit to eq 1 and gave k_{cat}/K_m values of 2.9 ×10^7 M^{-1} min^{-1} for wild-type cpFtsY, 4.8 ×10^6 M^{-1} min^{-1} for cpFtsY F71V, 3.7 ×10^6 M^{-1} min^{-1} for cpFtsY F71A, and 3.8 ×10^5 M^{-1} min^{-1} for cpFtsY G288W. Reactions contained 100 nM of cpSRP54 and varying concentrations of cpFtsY in the presence of 100 μM GTP. (C) Complex formation between cpSRP54 and wild-type cpFtsY (black) or mutant cpFtsY G288W (red) was monitored on Superdex 200. An arrow marks the position where the cpSRP54-cpFtsY complex appears. (D) Complex formation between cpSRP54 and wild-type cpFtsY (black) or mutant cpFtsY F71V (red) was monitored on Superdex 200. An arrow marks the position where the cpSRP54–cpFtsY complex appears.

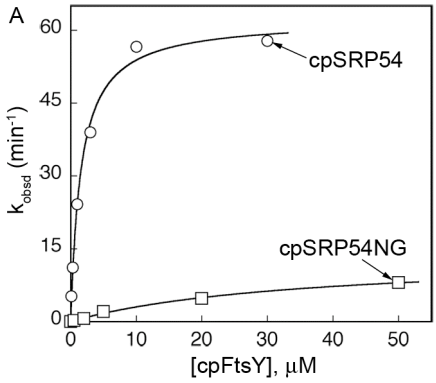

B

	NG	+M	+RNA
E. coli	(1)	2.2[a]	535[b]
chloroplast	5	587	395

Figure 2.3 The M-domain of cpSRP54 accelerates the interaction rate of cpSRP54 with cpFtsY. (A) Rate constants for the stimulated GTPase reactions of cpFtsY with cpSRP54 (○) or with cpSRP54 NG (□). The data were fit to eq 1, and the k_{cat}/K_m values are listed in Table 2.1. (B) Summary of the effect of M-domain and the SRP RNA on complex formation. The k_{cat}/K_m value of the reference reaction Ffh NG + FtsY → products was set to 1. The effect of the M-domain of Ffh[a] and of SRP RNA[b] has been previously reported ([a] from*31*, *33*; [b] from *26*).

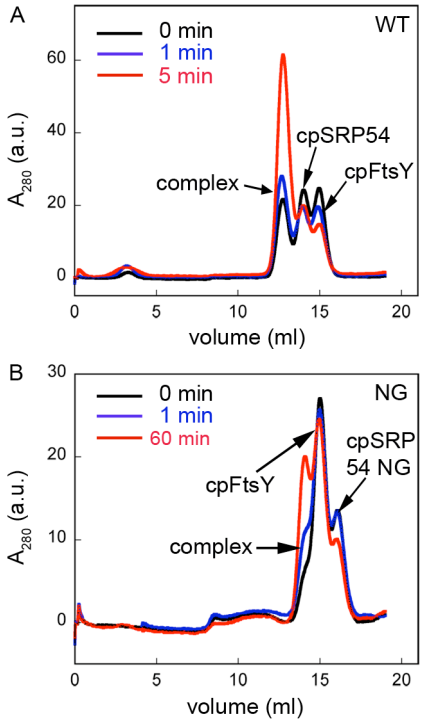

Figure 2.4 cpSRP54 NG is defective in complex formation. Complex formation between cpFtsY and full-length cpSRP54 (A) or cpSRP54 NG (B) was monitored on Superdex 200 as in Figure 2.2. Reactions were incubated for specified lengths of time before the protein mixtures were loaded onto the column.

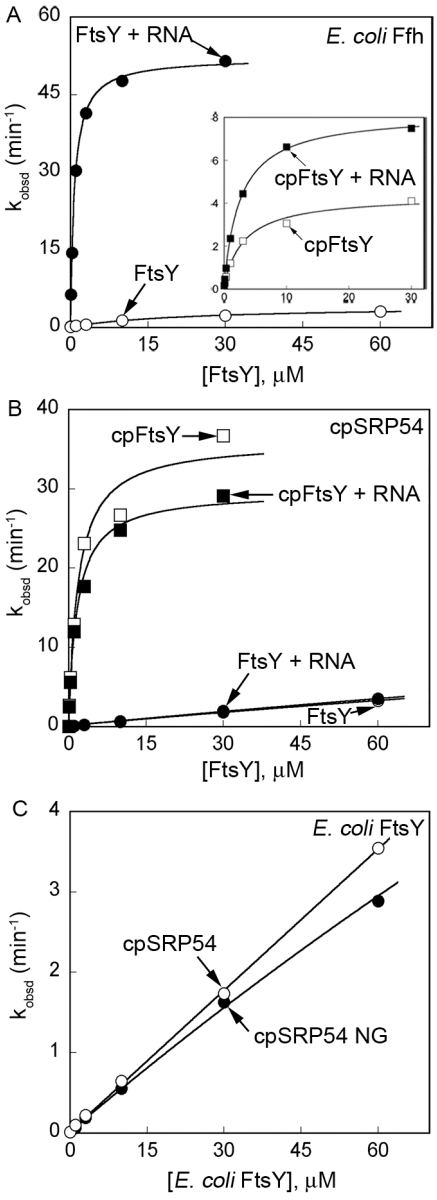

Figure 2.5 The stimulatory effect of the M-domain or the SRP RNA is specific to the SRP receptor in each pathway. (A) Rate constants for the stimulated GTPase reaction of *E. coli* Ffh with *E. coli* FtsY in the presence (●) or absence (○) of 4.5S SRP RNA, or with cpFtsY in the presence (■) or absence (□) of 4.5S SRP RNA (inset). (B) Rate constants for the stimulated GTPase reaction of cpSRP54 with *E. coli* FtsY in the presence (●) or absence (○) of 4.5S SRP RNA, or with cpFtsY in the presence (■) or absence (□) of 4.5S SRP RNA. (C) Rate constants for the stimulated GTPase reaction of *E. coli* FtsY with cpSRP54 (○) or cpSRP54 NG (●). The k_{cat}/K_m values were reported in Table 2.1.

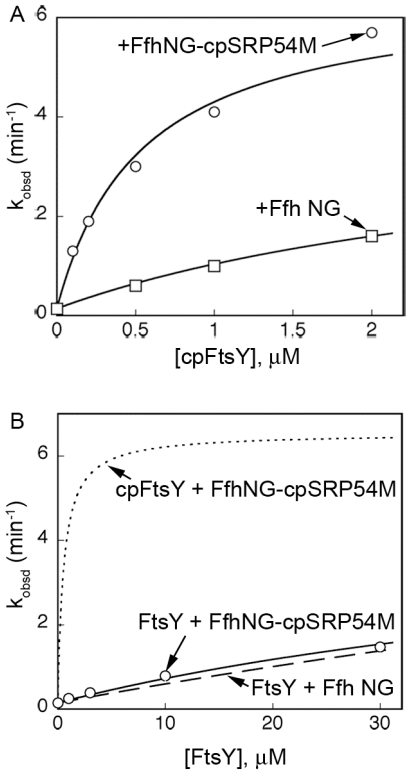

Figure 2.6 The M-domain of cpSRP54 can stimulate interactions with cpFtsY when fused to Ffh-NG. (A) Rate constants for the stimulated GTPase reaction of cpFtsY with the chimeric protein Ffh NG-cpSRP54 M (○) or Ffh NG (□). The data were fit to eq 1 and gave k_{cat}/K_m values of 1.2 ×10^7 M^{-1} min^{-1} for Ffh NG-cpSRP54 M and 7.4 ×10^5 M^{-1} min^{-1} for Ffh NG. Reactions contained 100 nM of FfhNG-cpSRP54M or 500 nM of FfhNG and varying concentrations of cpFtsY in the presence of 100 μM or 200 μM GTP, respectively. (B) The stimulatory effect of the cpSRP54 M-domain in the chimeric protein is specific to cpFtsY. The stimulated GTPase reaction of Ffh NG-cpSRP54M with *E. coli* FtsY (○) was determined as in part A, and nonlinear fits of the data to eq 1 gave k_{cat}/K_m values of 6.6 ×10^4 M^{-1} min^{-1}. The dotted line represents the reaction of the fusion protein with cpFtsY (from part A) and was shown for comparison. The dashed line represents the reaction of Ffh NG with *E. coli* FtsY (from Figure 2.1B) and was shown for comparison.

Supplementary Materials

Supplementary Table 2.S1 Kinetic constants for the basal GTPase activities of SRP and FtsY proteins used in this study

Protein construct	K_m (μM)	k_{max} (min^{-1})
Ffh[1]	0.3±0.05	0.093±0.002
Ffh NG	1.1±0.2	0.11±0.002
Ffh NG-cpSRP54 M	1.4±0.2	0.12±0.002
E. coli FtsY[1]	14±2	0.012±0.002
E. coli FtsY NG	9.0±3.7	0.0097±0.002
cpSRP54[2]	2.8±0.4	0.017±0.002
cpSRP54 NG	5.0±0.6	0.015±0.003
cpFtsY[2]	2.1±0.2	0.0045±0.002
cpFtsY F71V	0.3±0.07	0.004±0.0002
cpFtsY F71A	≤4.0	≤0.018
cpFtsY G288W	0.55±0.49	0.0068±0.0044

[1]These values have been previously reported in (*27*) and confirmed in this study.

[2]These values have been previously reported in (*26*) and confirmed in this study.

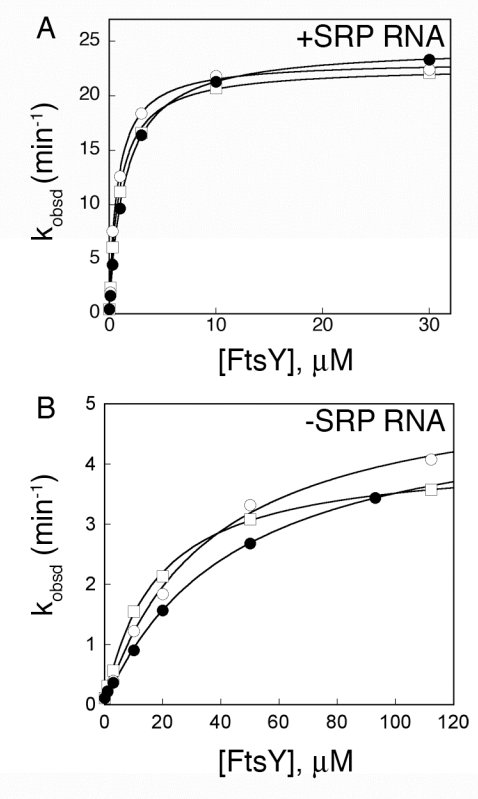

Supplementary Figure 2.S1 *E. coli* FtsY constructs with different N-terminal extensions exhibit similar reaction rates in the stimulated GTPase reactions with Ffh in the presence (A) or absence (B) of SRP RNA. Rate constants for the stimulated GTPase reaction of *E. coli* SRP or Ffh with *E. coli* FtsY NG (●), *E. coli* FtsY (47-497) (○) and *E. coli* FtsY full-length (□) were determined as described in Methods. In the case of SRP (A), the fit of the data to eq 1 gave k_{cat}/K_m values of 2.2 $\times 10^7$ M^{-1} min^{-1} for FtsY NG, 2.8 $\times 10^7$ M^{-1} min^{-1} for FtsY (47-497) and 1.5 $\times 10^7$ M^{-1} min^{-1} for full-length FtsY. In the case of Ffh (B), the fit of the data to eq 1 gave k_{cat}/K_m values of 1.2 $\times 10^5$ M^{-1} min^{-1} for FtsY NG, 1.5 $\times 10^5$ M^{-1} min^{-1} for FtsY (47-497) and 2.3 $\times 10^5$ M^{-1} min^{-1} for full-length FtsY.

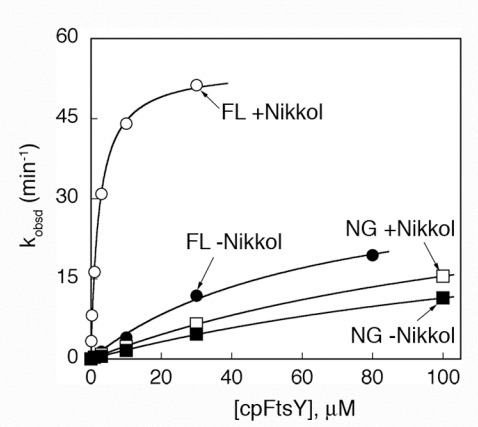

Supplementary Figure 2.S2 The stimulatory effect of cpSRP54 M-domain is observed only in the presence of Nikkol. Rate constants for the stimulated GTPase reactions were determined in the presence (open symbols) and absence (closed symbols) of 0.01% Nikkol with full-length cpSRP54 and cpSRP54-NG, and gave k_{cat}/K_m values of 2.4×10^7 and 2.6×10^5 M^{-1} min^{-1} for full-length cpSRP54 and cpSRP54-NG in the presence of Nikkol, respectively, and 5.4×10^5 and 1.9×10^5 M^{-1} min^{-1} for cpSRP54 and cpSRP54-NG in the absence of Nikkol, respectively.

References:

1. Walter, P., and Johnson, A. E. (1994) Signal sequence recognition and protein targeting to the endoplasmic reticulum membrane, *Ann. Rev. Cell Biol. 10*, 87–119.
2. Keenan, R. J., Freymann, D. M., Stroud, R. M., and Walter, P. (2001) The signal recognition particle, *Annu. Rev. Biochem. 70*, 755–775.
3. Walter, P., Ibrahimi, I., and Blobel, G. (1981) Translocation of proteins across the endoplasmic reticulum I. Signal Recognition Protein (SRP) binds to *in vitro* assembled polysomes synthesizing secretory protein, *J. Cell. Biol. 91*, 545–550.
4. Gilmore, R., Blobel, G., and Walter, P. (1982a) Protein translocation across the endoplasmic reticulum: 1. Detection in the microsomal membrane of a receptor for the signal recognition particle, *J. Cell Biol. 95*, 463–469.
5. Simon, S. M., and Blobel, G. (1991) A protein-conducting channel in the endoplasmic reticulum, *Cell 65*, 371–380.
6. Gorlich, D., Prehn, S., Hartmann, E., Kalies, K. U., and Rapoport, T. A. (1992) A mammalian homolog of Sec61p and SecYp is associated with ribosomes and nascent polypeptides during translocation, *Cell 71*, 489–503.
7. Halic, M., Blau, M., Becker, T., Mielke, T., Pool, M.R., Wild, K., Sinning, I., and Beckmann, R. (2006) Following the signal sequence from ribosomal tunnel exit to signal recognition particle, *Nature 444* 507–511.
8. Powers, T., and Walter, P. (1995) Reciprocal stimulation of GTP hydrolysis by two directly interacting GTPases, *Science 269*, 1422–1424.
9. Connolly, T., Rapiejko, P. J., Gilmore, R. (1991) Requirement of GTP hydrolysis for dissociation of the signal recognition particle from its receptor, *Science 252*, 1171–1173.
10. Freymann, D. M., Keenan, R. J., Stroud, R. M., and Walter, P. (1997) Structure of the conserved GTPase domain of the signal recognition particle, *Nature 385*, 361–364.
11. Montoya, G., Svensson, C., Luirink, J., and Sinning, I. (1997) Crystal structure of the NG domain from the signal recognition particle receptor FtsY, *Nature 385*, 365–368.
12. Batey, R. T., Rambo, R. P., Lucast, L., Rha, B., and Doudna, J. A. (2000) Crystal structure of the ribonucleoprotein core of the signal recognition particle, *Science 287*, 1232–1239.
13. Zopf, D., Bernstein, H. D., Johnson, A. E., and Walter, P. (1990) The methionine-rich domain of the 54 kd protein subunit of the signal recognition particle contains an RNA binding site and can be crosslinked to a signal sequence, *EMBO J. 9*, 4511–4517.
14. Parlitz, R., Eitan, A., Stjepanovic, G., Bahari, L., Bange, G., Bibi, E., and Sinning, I. (2007) *Escherichia coli* signal recognition particle receptor FtsY contains an essential and autonomous membrane-binding amphipathic helix, *J Biol Chem. 282*, 32176–32184.

15. Angelini, S., Deitermann, S., and Koch, H.G. (2005) FtsY, the bacterial signal-recognition particle receptor, interacts functionally and physically with the SecYEG translocon, *EMBO Rep. 6*, 476–481.
16. Shan, S., and Walter, P. (2003) Induced Nucleotide Specificity in a GTPase, *Proc. Natl. Acad. Sci. U.S.A. 100*, 4480–4485.
17. Focia, P. J., Shepotinovskaya, I.V., Seidler, J.A., and Freymann, D.M. (2004) Heterodimeric GTPase Core of the SRP Targeting Complex, *Science 303*, 373–377.
18. Egea, P. F., Shan, S., Napetschnig, J., Savage, D.F., Walter, P., and Stroud, R.M. (2004) Substrate twinning activates the signal recognition particle and its receptor, *Nature 427*, 215–221.
19. Neher, S. B., Bradshaw, N., Floor, S.N., Gross, J.D., Walter, P. (2008) SRP RNA controls a conformational switch regulating the SRP-SRP receptor interaction, *Nat Struct Mol Biol. 15*, 916–923.
20. Shan, S., Stroud, R., Walter, P. (2004) Mechanism of association and reciprocal activation of two GTPases, *PLoS Biology 2*, e320.
21. Schuenemann, D., Gupta, S., Persello-Cartieaux, F., Klimyuk, V. I., Jones, J. D. G., Nussaume, L., and Hoffman, N. E. (1998) A novel signal recognition particle targets light-harvesting proteins to the thylakoid membranes, *Proc. Natl. Acad. Sci. USA 95*, 10312–10316.
22. Tu, C. J., Peterson, E. C., Henry, R., and Hoffman, N. E. (2000) The L18 domain of light-harvesting chlorophyll proteins binds to chloroplast signal recognition particle 43, *J. Biol. Chem. 275*, 13187–13190.
23. Delille, J., Peterson, E. C., Johnson, T., Morre, M., Kight, A., and Henry, R. (2000) A novel precursor recognition element facilitates posttranslational binding to the signal recognition particle in chloroplasts, *Proc. Natl. Acad. Sci. 97*, 1926–1931.
24. Groves, M. R., Mant, A., Kuhn, A., Koch, J., Dubel, S., Robinson, C., and Sinning, I. (2001) Functional characterization of recombinant chloroplast signal recognition particle, *J. Biol. Chem. 276*, 27778–27786.
25. Goforth, R. L., Peterson, E.C., Yuan, J., Moore, M.J., Kight, A.D., Lohse, M.B., Sakon, J., and Henry, R.L. (2004) Regulation of the GTPase cycle in post-translational signal recognition particle-based protein targeting involves cpSRP43, *J. Biol. Chem. 279*, 43077–43084.
26. Jaru-Ampornpan, P., Chandrasekar, S., Shan, S. (2007) Efficient interaction between two GTPases allows the chloroplast SRP pathway to bypass the requirement for an SRP RNA, *Mol Biol Cell. 18*, 2636–2645.
27. Peluso, P., Shan, S., Nock, S., Herschlag, D., and Walter, P. (2001) Role of SRP RNA in the GTPase cycles of Ffh and FtsY, *Biochemistry 40*, 15224–15233.
28. Zhang, X., Kung, S., and Shan, S. (2008) Demonstration of a multistep mechanism for assembly of the SRP- SRP receptor complex: implications for the catalytic role of SRP RNA., *J Mol Biol. 381(3)*, 581–593.
29. Peluso, P., Herschlag, D., Nock, S., Freymann, D. M., Johnson, A. E., and Walter, P. (2000) Role of 4.5S RNA in assembly of the bacterial signal recognition particle with its receptor, *Science 288*, 1640–1643.

30. Siu, F. Y., Spanggord, R.J., and Doudna, J.A. (2007) SRP RNA provides the physiologically essential GTPase activation function in cotranslational protein targeting, *RNA 13*, 240–250.
31. Bradshaw, N., and Walter, P. (2007) The signal recognition particle (SRP) RNA links conformational changes in the SRP to protein targeting, *Mol Biol Cell 18*, 2728–2734.
32. Bradshaw, N., Neher, S.B., Booth, D.S., and Walter, P. (2009) Signal sequences activate the catalytic switch of SRP RNA, *Science 323*, 127–130.
33. Chandrasekar, S., Chartron, J., Jaru-Ampornpan, P., and Shan, S. (2008) Structure of the chloroplast signal recognition particle (SRP) receptor: domain arrangements govern the SRP-receptor interaction, *J Mol Biol 375*, 425–436.
34. Shepotinovskaya, I. V., and Freymann, D. M. (2001) Conformational change of the N-domain on formation of the complex between the GTPase domains of *Thermus aquaticus* Ffh and FtsY, *Biochemica et Biophysica Acta 1597*, 107–114.
35. Richter, C. V., Träger, C., and Schünemann, D. (2008) Evolutionary substitution of two amino acids in chloroplast SRP54 of higher plants cause its inability to bind SRP RNA, *FEBS Lett. 582*, 3223–3229.
36. Schaffitzel, C., Oswald, M., Berger, I., Ishikawa, T., Abrahams, J.P., Koerten, H.K., Koning, R.I., and Ban, N. (2006) Structure of the E. coli signal recognition particle bound to a translating ribosome, *Nature 444*, 503–506.
37. Jagath, J. R., Matassova, N. B., de Leeuw, E., Warnecke, J. M., Lentzen, G., Rodnina, M. V., Luirink, J., and Wintermeyer, W. (2001) Important role of the tetraloop region of 4.5S RNA in SRP binding to its receptor FtsY, *RNA 7*, 293–301.
38. Zheng, N., and Gierasch, L.M. (1997) Domain interactions in E. coli SRP: stabilization of M domain by RNA is required for effective signal sequence modulation of NG domain, *Mol Cell 1*, 79–87.
39. Zhang, X., Schaffitzel, C., Ban, N., and Shan, S. (2009) Multiple conformational switches in a GTPase complex control co-translational protein targeting, *Proc. Natl. Acad. Sci. USA 106*, 1754–1759